PALEOSEISMOLOGICAL STUDY IN THE ST. LOUIS REGION: COLLABORATIVE RESEARCH, M. TUTTLE & ASSOCIATES AND THE EASTERN REGION CLIMATE/HAZARDS TEAM, USGS

Final Technical Report

Research supported by the U.S. Geological Survey
award 1434-99HQGR0032

Martitia P. Tuttle
M. Tuttle & Associates
Georgetown, ME 04548
Tel: 207-371-2796
e-mail: mptuttle@earthlink.net

Program Element II: Research on Earthquake Occurrence and Effects

Key Words: Paleoseismology, Paleoliquefaction, Recurrence Interval, Age Dating

The views and conclusions contained in this document are those of the authors and should not be interpreted as necessarily representing the official policies, either expressed or implied, of the U.S. Government.

PALEOSEISMOLOGICAL STUDY IN THE ST. LOUIS REGION

Abstract

At least two generations of Holocene earthquake-induced liquefaction features, including sand and silt dikes and sills and only two sand blows, occur in the St. Louis region. Some of these features probably formed during the 1811-1812 New Madrid earthquakes and others formed during a Middle Holocene earthquake in 4,520 B.C. ± 160 yr. Liquefaction features along the Meramec River south of St. Louis formed since A.D. 1670, probably during the 1811-1812 earthquakes. Other Late Holocene sand dikes, ranging up to 26 cm in width, occur along the Kaskaskia River and its tributaries Crooked, Shoal, and Silver Creeks, as well as along Cahokia and Piasa Creeks and the Cache, Castor, Marys, and Meramec Rivers. The 1811-1812 New Madrid earthquakes, or similar events in A.D. 1450, A.D. 900, and A.D. 300, may have been responsible for these Late Holocene liquefaction features in the St. Louis region. Middle Holocene liquefaction features, including two sand blows and numerous sand dikes, ranging up to 45 cm in width, occur along the Kaskaskia River and its tributaries Crooked, Mud, and Shoal Creeks, as well as along Cahokia Creek and the Big Muddy and Cache Rivers. The 4,520 B.C. ± 160 yr earthquake may or may not have been responsible for all these Middle Holocene features. The relatively large size of some of these features near Germantown, Illinois, suggests that the earthquake source may be located east of St. Louis. However, the location and magnitude of the Middle Holocene event remains uncertain. Additional work is needed to better constrain the ages of liquefaction features and thus the timing of the earthquakes that caused them, and to correlate similar-age liquefaction features across the region and thus further define the extent of liquefaction during each event.

Introduction

Through the use of liquefaction features, great strides have been made in elucidating the record of prehistoric earthquakes in the central United States. For example, it is now recognized that the New Madrid seismic zone (NMSZ) generated very large (**M** ≥ 7.6) prehistoric earthquakes circa A.D 1450 ± 150 yr and A.D. 900 ± 100 yr (Tuttle et al., 2002), as well as other significant events circa A.D. 300 ± 200 yr and 2350 B.C. ± 200 yr (e.g., Saucier, 1991; Tuttle et al., 2005). The Wabash Valley seismic zone (WVSZ) in southeastern Illinois, and southwestern Indiana, has been interpreted as the source of a **M** 7.2-7.8 earthquake circa 6,100 ± 200 radiocarbon yr B.P. and a **M** 7.1-7.3 event circa 12,000 ± 1000 radiocarbon yr B.P. (e.g., Obermeier et al., 1993; Munson et al., 1997; Olson et al., 2004). Other prehistoric earthquakes have been inferred from paleoliquefaction features located far from recognized seismic zones, including an earthquake of **M** 6.2-6.8 near Springfield between 5,900-7,400 radiocarbon yr B.P. (e.g., Hajic and Wiant, 1997; McNulty and Obermeier, 1999). Also, liquefaction features have been found in the St. Louis region suggesting strong ground shaking at least twice during the past 6,500 years (e.g., McNulty and Obermeier, 1999; Tuttle et al., 1998, 1999). Nevertheless, questions remain regarding the number, source areas, and magnitude of earthquakes that induced liquefaction in this region during the Holocene. This report presents results of a paleoseismic study in the St. Louis region designed to pickup where previous studies had left off in an attempt to address these outstanding questions regarding paleoearthquakes.

Geological and Seismological Setting

The St. Louis region straddles the Mississippi River and includes the eastern portion of the Ozark uplift and western portion of the Illinois basin (Fig. 1). The Illinois basin was initiated in the Early Paleozoic and experienced episodes of rapid sediment accumulation during the Late Cambrian and Mississippian (e.g, Quinlan, 1987). The Ozark uplift originated in the Precambrian and experienced several episodes of uplift and sedimentation during the Paleozoic (e.g., McCracken, 1971). Youthful topographic features in the Ozarks indicate renewed uplift during the Quaternary. Well-known geologic structures in the region include the St. Louis and Centralia faults, the Valmeyer and Waterloo-Dupo anticlines, and the Du Quoin monocline (Fig. 1).

The St. Louis region is characterized by low to moderate seismic activity, in stark contrast to the highly active NMSZ to the south (Fig. 1; Nuttli and Brill, 1981; Johnston and Schweig, 1996). A diffuse concentration of seismicity extends northwest from the NMSZ to the St. Louis region. Seismicity in this region is thought to be caused by reactivation of old basement faults. Although several earthquakes have been spatially associated with the St. Louis fault (e.g., Harrison, 1997) and the Centralia fault zone (Mitchell et al., 1991), no earthquake has been directly attributed to any particular geologic structure (Fig. 1).

Results of Previous Paleoseismology Studies in the St. Louis Region

In the mid-1990s, liquefaction features were found along the Kaskaskia River east of St. Louis (Obermeier, pers. comm., 1995). This finding prompted two paleoseismology studies in the St. Louis region to determine if the liquefaction features formed as a result of large earthquake(s) produced by a local source or very large earthquakes centered in the New Madrid or Wabash Valley seismic zones.

In a study focused in the area east of St. Louis, two generations of sand dikes, including a 45-cm-wide dike, were found along Kaskaskia River and its tributary Shoal Creek (McNulty and Obermeier, 1999). The study concluded that a **M** > 6 earthquake occurred near the lower portion of Shoal Creek during the Middle Holocene about 6,500-7,000 radiocarbon yr B.P. The age of the event was estimated from the weathering characteristics of sand dikes and dating of deposits cut by the dikes. The earthquake source area was inferred from the local distribution of liquefaction features. The magnitude of the earthquake was derived from the relation between earthquake magnitude and maximum epicentral distance to surface evidence of liquefaction (e.g., Ambraseys, 1988).

In a regional paleoseismology study conducted by the PI for the U.S. Nuclear Regulatory Agency, more than 400 km of rivers and creeks were surveyed across southeastern Missouri and southwestern Illinois for evidence of Quaternary faulting or folding and earthquake-induced liquefaction (Figs. 1 and 2; Tuttle et al., 1998 and 1999). At least two generations of liquefaction features, including two sand blows and many sand and silt dikes and sills, were found along the Big Muddy, Cache, Castor, Marys, Meramec and Kaskaskia Rivers and Mud, Shoal, and Silver Creeks. The sand blows, as well as a few truncated sand dikes, provided minimum age constraints, in addition to maximum age constraints. Thus, age estimates were narrowly

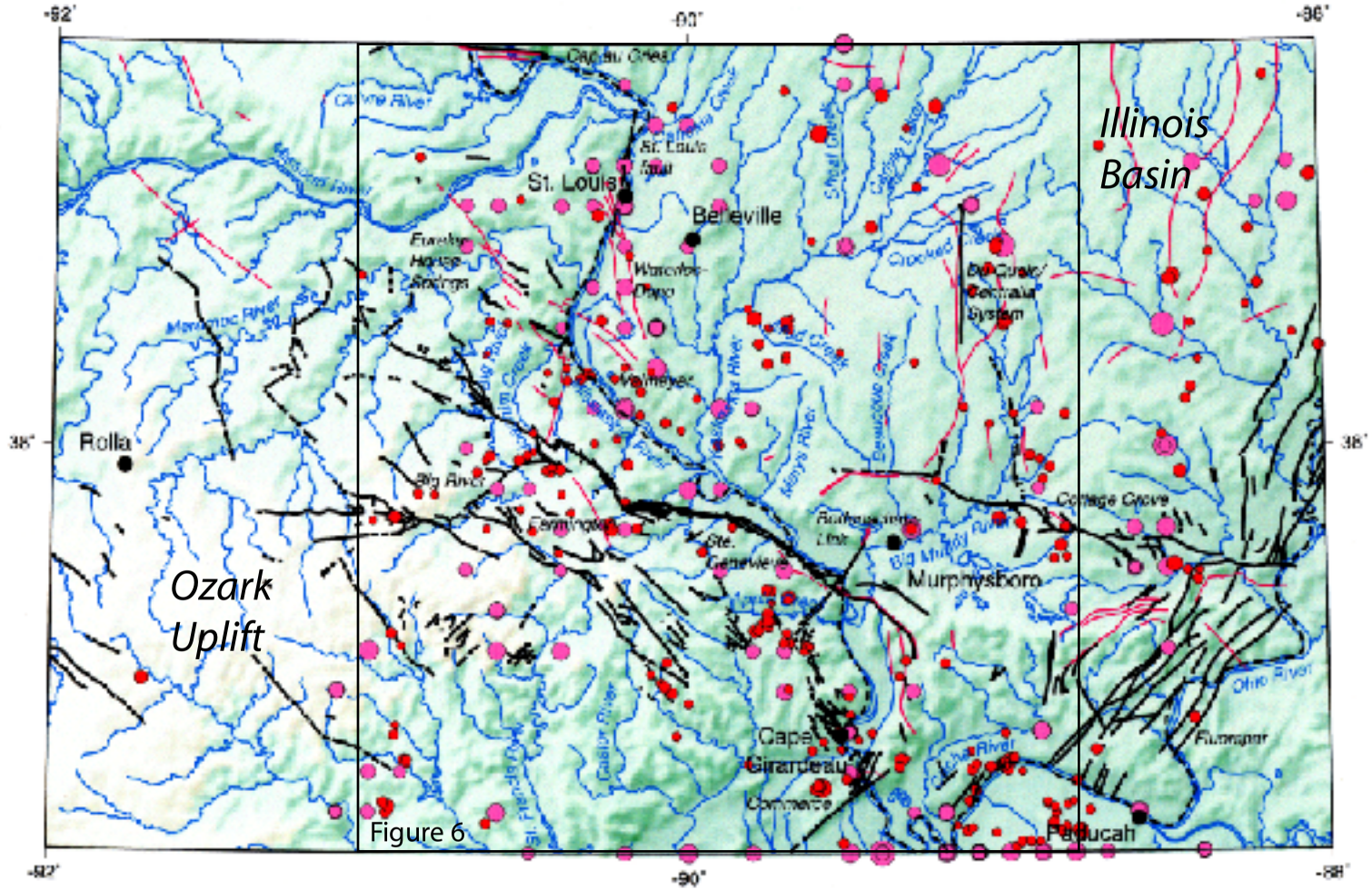

Figure 1. Seismicity and structural features on topographic-hydrographic map of area of southeastern Missouri and southwestern Illinois (from Tuttle et al., 1999). Red circles show epicenters of magnitude 2.0 or greater earthquakes recorded by Central Mississippi Valley Seismic Network between 1927 and 1999. Pink circles show epicenters of historical seismicity of magnitude 2.0 or greater prior to 1972 (Nuttli and Brill Catalog, 1981). Symbol size increases with magnitude. Surface traces of faults and folds are shown with heavy and thin black lines, respectively. Area of St. Louis regional paleoseismology study is outlined above and shown in Figure 2.

constrained for several liquefaction features, and thus for their causative earthquakes. Sand dikes at two sites on the Meramec River appeared to have formed during the 1811-1812 earthquakes and two sand blows and several sand dikes on the Kaskaskia River and Shoal Creek werre estimated to have formed in 4520 B.C. ± 160 yr or 6,500 B.P. (also 5,670 ± 80 radiocarbon yr B.P.). Although they were assigned to general age classes (e.g., Late Holocene, Middle Holocene, Holocene, or Late Wisconsin-Holocene), most of the other liquefaction features have poor age constraints, making regional correlation problematic. In addition, the liquefaction potential of sandy layers represented in borehole logs from fourteen bridge sites the region was determined for earthquakes of **M** 5.25, 6.0, 6.75, and 7.5 at distances of 10, 32, 40, 80, 100, and 125 km (Tuttle et al., 1999). On the basis of the analysis, it was proposed that several different earthquake scenarios could explain the observed distribution of liquefaction features. The earthquake scenarios serve as working hypotheses to be tested through additional fieldwork and liquefaction analysis.

Investigations Undertaken

The main goals of this study are to constrain the age estimates of earthquakes that induced liquefaction in the St. Louis region and to gain additional information about the size and spatial distribution of similar-aged liquefaction features. In order to achieve these goals, we searched areas not previously surveyed for liquefaction features, documented and dated liquefaction features in those areas, studied in detail a liquefaction site in the suburbs of St. Louis, conducted liquefaction potential analysis of borehole data collected at that site by the Missouri Department of Transportation, and evaluated the age estimates of liquefaction features found during this study and those found during a previous study funded by the U.S. Nuclear Regulatory Commission. The overall purpose of this research is to improve our understanding of the earthquake hazard of the St. Louis region. This project was conducted in collaboration with Eugene Schweig of the U.S. Geological Survey. John Sims, Ingrid Ekstrom, Dave Hoffman assisted with river reconnaissance. John Sims participated in logging of liquefaction features at site MR25W. Kathleen Dyer-Williams performed the liquefaction potential analysis.

Results of Investigations

River Reconnaissance and Newly Found Liquefaction Features

During this study, reconnaissance for liquefaction features was conducted along rivers and creeks in the St. Louis region. They include the Cuivre, Meramec, and Missouri Rivers and Femme Osage and Saline Creeks in southeastern Missouri, and the Cache and Kaskaskia Rivers and Cahokia, Crooked, Fountain, Horse, Piasa, Prairie du Pont, Richland, Shoal, and Silver Creeks in southwestern Illinois (Fig. 2). Brief descriptions of conditions encountered along these rivers and streams are given below.

We found no additional liquefaction features along the Cache, Cuivre and Missouri Rivers or along the Femme Osage, Fountain, Horse, Prairie du Pont, Richland, Saline and Silver Creeks. However, we did find and document thirty additional sand and silt dikes along Meramec and Kaskaskia Rivers and the Cahokia, Crooked, Piasa, and Shoal Creeks. The locations, sizes, orientations, and estimated ages of the sand dikes are summarizes in Table 1.

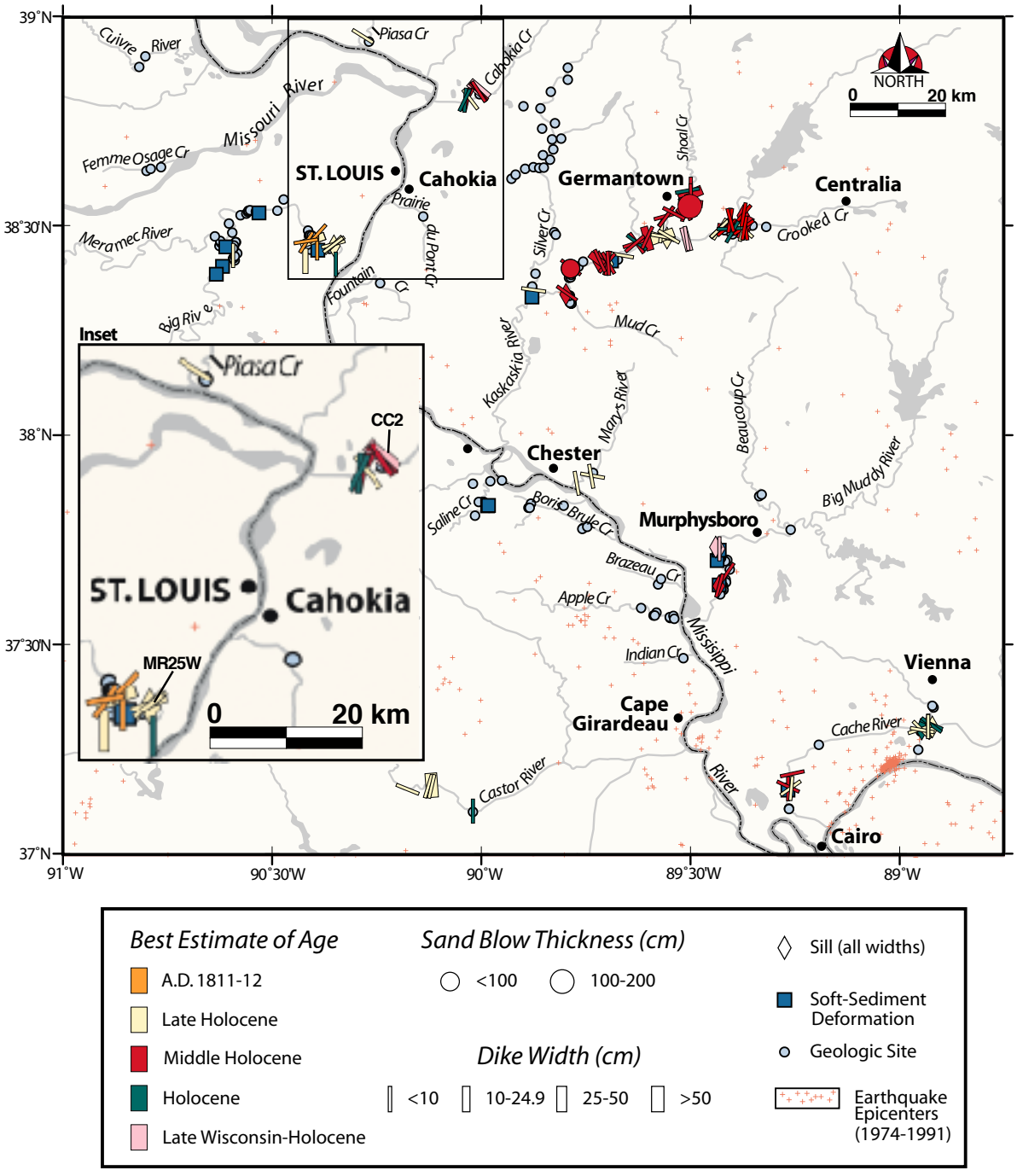

Figure 2. Earthquake-induced liquefaction features documented during this project and prior paleoseismological study in St. Louis region (Tuttle et al., 1998, 1999). Inset shows blowup of outlined St. Louis area. Ages of few liquefaction features are well-constrained making it difficult to estimate timing, locations, and magnitudes of causative earthquakes. McNulty and Obermeier (1999) also reported liquefaction features along portions of Kaskaskia River and Shoal Creek.

At the liquefaction sites, as well as other nearby sites, we collected organic samples for dating purposes. The PI selected a few of the samples for radiocarbon dating, which was performed by Beta Analytic, Inc. Results of radiocarbon dating are presented in Table 2. Based on the radiocarbon results and the observed weathering characteristics of the sand dikes, the PI estimated the ages of the liquefaction features and graded the age estimate (see Appendix I). Sand dikes at Meramec River site 203 formed since A.D. 1670, probably during the 1811-1812 New Madrid earthquakes. Other dikes that may be Late Holocene in age occur on Kaskaskia and Meramec Rivers and Cahokia, Crooked, and Piasa Creeks. Sand dikes at Kaskaskia River site 200 (KR200) formed since 7495 B.C., possibly during the 4520 B.C. ± 160 yr event. Other dikes that may be Middle Holocene in age occur on the Kaskaskia River and Cahokia and Crooked Creeks.

Cache River

Downstream from Ullin, Illinois, we surveyed 12 km of the Cache River, a former tributary to the Ohio River. Exposure was poor along most of this portion of the river due to beaver dams, channelization, and heavy vegetation. The few exposures revealed mottled clayey silt. Probing at several sites, we found interbedded silt and sand below river level. We found no liquefaction features along this portion of the Cache River; however this is not surprising given the poor exposure.

Cahokia Creek

Downstream from Edwardsville, Illinois, we surveyed 8 km of Cahokia Creek, a tributary to the Mississippi River. This portion of the creek is incised into the uplands and crosses the eastern margin of the Mississippi River floodplain. Exposure was good and cutbanks range from 3 to 11 m in height. Sediment profiles include buff-colored and rose-colored silt overlying either reddish silt containing calcium carbonate nodules or rythmites of silt and sand and mottled silt overlying interbedded silt and fine sand. Probing at several sites indicates thicker beds of coarse to medium sand below the water level.

We found nine sand dikes at five different sites along Cahokia Creek (see Fig. 2 and Table 1). The widest sand dike is located at site 2 (CC2 on Fig. 2; Fig. 3) about 25 km northeast of St. Louis. The sand dike is 35-cm wide, crosscuts a sandy layer, and intrudes and terminates within a diamicton (probably a glacial till) overlain by what appears to be Roxanna loess (60-26 ky). The dike fines upward from pebbly, coarse to medium sand. Fines (silt and clay) have accumulated in the upper portion of the dike and the entire feature is either iron-cemented or iron-stained. The weathering characteristics of the large sand dike indicate that it is prehistoric in age and are similar to those in Middle Holocene sand dikes. Given that it intrudes a glacial deposit, the sand dike clearly formed during or since the Wisconsin.

The other sand dikes along the creek range from 0.5 to 6 cm in width. Sand dikes at sites 4 and 6 are very weathered and interpreted as Middle Holocene in age. In contrast, the sand dike at site 5 is loose, unweathered, and appears to be young. Radiocarbon dating of wood from a tree trunk bedded in silt about 54 cm below the dike termination indicates that it formed since 160 B.C. or during the Late Holocene.

Table 1. Liquefaction features found during river reconnaissance in St. Louis region.

River Site #	Latitude	Longitude	Sand Dike Width (cm)	Strike and Dip	Age Estimate
Cahokia Ck.					
2	38.82718	90.00360	35	N50°W, 85°SW	Late Wisconsin-Holocene
4	38.82413	90.00697	1.25 1 0.5	N33°W, 84°NE N38°W, 87°NE N47°W, 90°	Middle Holocene
5	38.80654	90.02695	1.5	N37°W, 88°NE	Late Holocene
6	38.80519	90.03262	1.5 1	N13°E, 88°NW N28°E, 88°SE	Middle Holocene
7	38.80485	90.03696	6 4	N26°E, 64°NW N4°E, 75°SE	Holocene
Crooked Ck.					
4	38.5005	89.3660	14	N28°E, vertical	Middle Holocene
5	38.4995	89.3684	4	N8°W, 89°W	Middle Holocene
6	38.4994	89.3703	6 2	N10°E, 86°NW N55°E, 85°NW	Middle Holocene
7	38.4957	89.3725	1.5 1.5	N15°E, 87°SE N48°W, vertical	Late Holocene
8	38.4894	89.3978	5	N30°E, 80°NW	Holocene
9	38.4954	89.4038	3.5	N88°E, 80°SE	Holocene
Kaskaskia R.					
200	38.5311	89.3718	7 3	N10°E, 85°SE N40°E, 72°NW	Middle Holocene
201	38.5175	89.4044	6 4	N15°W, 78°SW N9°E, 84°NW	Middle Holocene
201	38.5175	89.4044	3	N3°E, 85°SE	Late Holocene
Meramec R.					
25W	38.4585	90.3507	20 1 1	N70°E, 86°NW N52°E, 78°NW N45°E, 87°SE	Late Holocene
203	38.4651	90.4152	8 6	N81°E, 65°SE N32°E, 82°NW	1811-1812
Piasa Ck.					
2	38.95698	90.28497	1.5	N58°W, 85°SW	Late Holocene
Shoal Ck.					
100	38.5924	89.4982	1, 1		Holocene
101	38.5866	89.5033	3	N80°E, 80°SE	Holocene

Table 2. Results of radiocarbon analysis of samples from sites in St. Louis region.

Site-Sample Lab-Sample	$^{13}C/^{12}C$ Ratio	Radiocarbon Age[1]	Calendar Yr [2]	Sample Description
Cahokia Ck 3-W1 Beta-171815	-28.8	1320 ± 80	A.D. 600-890	Leaves 1.4 m below surface and 1.8 m above WL
Cahokia Ck 5-W2 Beta-171816	-26.5	2000 ± 60	160 B.C.-A.D. 120	Wood 3 m below surface from outer part of tree trunk
Crooked Ck 4-W1 Beta-142694	-26.4	121.6 ± 0.6%	Modern	Wood 3.43 m below surface and 28 cm below dike tip
Crooked Ck 7-C2 Beta-142695	-24.1	5820 ± 50	4785-4540 B.C.	Charcoal from weathered silt 11 cm below dike tip
Fountain Ck 1-C1 Beta-171817	-27.5	160 ± 40	A.D. 1660-1950	Charcoal 2.55 m below surface from top of paleosol
Femme O. Ck 1-W1 Beta-171818	-28.1	3890 ± 70	2570-2520 B.C. 2500-2140 B.C.	Leaves 10-20 cm above water level (WL)
Kaskaskia R 200-W1 Beta-142697	-28.2	8250 ± 70	7495-7070 B.C.	Wood 2.7 m below dike tip and 5.2 m below surface
Meramec R 25-W1003 Beta-159783	-25.1	5360 ± 70	4340-3990 B.C.	Wood 1.55 m below dike tip and 5.21 m below surface
Meramec R 25-C1000 Beta-159782	-25.6	5490 ± 40	4370-4250 B.C.	Charcoal 1.45 m below dike tip and 5.11 m below surface
Meramec R 25-W1 Beta-142698	-27.1	5510 ± 40	4440-4320 B.C.	Wood 2 m below dike tip and 5.66 m below surface
Meramec R 202-C1 Beta-142699	-26.0	2510 ± 50	800-415 B.C.	Charcoal 3.28 m below surface from shell midden
Meramec R 203-C1 Beta-142700	-25.1	110 ± 40	A.D. 1670-1780 A.D. 1795-1955	Charcoal adjacent to dike tip
Piasa Ck 1-W2 Beta-171819	-26.6	110 ± 60	Outside calibration range	Wood 1 m below surface from outer part of tree trunk
Piasa Ck 2-W1 Beta-171820	-26.8	106.9 ± 0.5%	Modern	Organics 14 cm above dike tip
Prairie du P. Ck 1-W1 Beta-171821	-27.5	430 ± 60	A.D. 1410-1530 A.D. 1550-1630	Leaves and debris 1m above WL from channel fill
Shoal Ck 102-W1 Beta-142702	-29.7	220 ± 60	A.D. 1515-1590 A.D. 1620-1705 A.D. 1715-1885 A.D. 1910-1950	Wood 4.5 m below surface and 0.5 m above WL from outer part of tree trunk in organic layer

[1] 1-sigma conventional radiocarbon ages in years B.P. or before present (1950) determined by Beta Analytic, Inc.
[2] 2-sigma calibrated age ranges in calendar years determined by Beta Analytic, Inc., using the Pretoria procedure (Talma and Vogel, 1993; Vogel *et al*., 1993).

Figure 3. (Left) View of cutbank along Cahokia Creek where 35 cm wide pebbly, sand dike was found about 25 km northeast from downtown St. Louis. Sand dike intrudes, and therefore post-dates, Wisconsin age deposits. Strike of sand dike is sub-parallel to nearby bluff suggesting that local topography may have influenced ground failure and enhanced dike width. (Right) Close-up of upper part of sand dike. Weathering characteristics, such as fines accumulation and iron-staining, indicate that sand dike is prehistoric in age and similar to Middle Holocene sand dikes found elsewhere in the region. Photos by M. Tuttle.

Crooked Creek

We surveyed the lowermost 33 km of Crooked Creek, a tributary to the Kaskaskia River. There was good exposure along the entire length of the creek. The Crooked Creek valley is only about 1-2 km wide. Where it flowed along the valley margin, the creek has tall cutbanks exposing diamicton or rythmites of silt and clay. Within the valley, cutbanks range from 3 to 6 m in height and expose primarily mottled silt. Along the lower 10 km of the creek, we found 8 dikes at 6 different sites (see Fig. 2 and Table 1). The dikes range from 1.5 to 14 cm in width and several of them are composed of silt rather than sand. At site 7, charcoal collected from mottled silt 11 cm below the termination of a sand dike indicates that it formed since 4785 B.C (Table 2). The sand dikes at this site exhibite no weathering or soil development and therefore are interpreted to be Late Holocene in age. Dikes at sites 4,5, and 6, however, are quite weathered up to 45 cm below their terminations. These dikes are interpreted as Middle Holocene in age.

Cuivre River

We surveyed the lowermost 25 km of the Cuivre River, a tributary to the Mississippi River. In general, exposure was poor and sedimentary conditions did not appear especially conducive to the formation of liquefaction features. Due to channelization, exposure was almost non-existent along the lowermost 5 km of the river, where it crosses the Mississippi River floodplain. The uppermost 12 km of the river meanders across a narrow valley, ranging from 0.5 to 1.5 km in width. Bedrock is exposed where the river flows near the valley margins. There are few exposures of interbedded silt and sand along this portion of the river. Along the middle portion of the river, we observed a few exposures of mottled silt or interbedded silt and sand. We found no liquefaction features along Cuivre River.

Femme Osage Creek

We surveyed the lowermost 10 km of Femme Osage Creek, a tributary to the Missouri River. This portion of the creek is incised in the uplands near Defiance, Missouri, and crosses the floodplain of the Missouri River. Exposure is poor for the entire length of the creek but is especially bad along the lower 2.5 km, where the creek has been channelized. In the upper reaches, bedrock is exposed in a few locations. Elsewhere, there are several 3 to 5 m high exposures of brownish silt overlying either layered silt or interbedded silt and sand. We found no liquefaction features along this creek.

Fountain Creek

We surveyed 4 km of Fountain Creek, a tributary to the Mississippi River, where it is incised in the uplands east of the Mississippi River floodplain. Exposure was poor and limited to bedrock outcrops and 3 to 4 m cutbanks of mottled silt overlying reddish silt. Conditions are not suitable along this creek for the formation of liquefaction features.

Horse Creek

We conducted reconnaissance on foot and by car along the lower 5 km of Horse Creek, a tributary to the Kaskaskia River. The creek banks are low and poorly exposed. In addition, the water level was fairly high, apparently backed up from the Kaskaskia River. We concluded that little or no information about past earthquakes could be obtained from a closer survey of the creek

Kaskaskia River

We surveyed 26 km of the Kaskaskia River downstream from Carlyle Reservoir. At the time the upper 18 km of the river was searched, the river level was high due to release of water from the reservoir and therefore exposure was poor. During reconnaissance of the lower 8 km, the river level was low and exposure was very good. Where the river flowed along the valley margin, bedrock or diamicton was exposed. Where the river crosses the valley, howver, cutbanks were usually 5 to 6 m high and revealed mottled silt overlying interbedded silt and sand or sand. We found and documented two liquefaction sites with multiple sand dikes along this portion of the river (see Fig. 2 and Table 1).

Meramec River

The PI had found sand dikes along the Meramec River during a previous study. We resurveyed the lower 22 km of the Meramec River with the hope that additional liqufaction features had been exposed by cutbank erosion. We found one additional liquefaction site about 300 m upstream from the Highway 21 bridge near Paulina Hills, Missouri (see Fig. 2 and Table 1). The liquefaction feature at this site is an upward branching sand dike. Radiocarbon dating of charcoal collected adjacent to the uppermost dike tip indicates that it formed since A.D. 1670 (Table 2). Only the 1811-1812 New Madrid earthquakes are known to have induced liquefaction in the St. Louis area. Therefore, we expect that this sand dike also formed in 1811-1812.

Missouri River

We surveyed by motorboat 15 km of the Missouri River in the vicinity and upstream from St. Charles, Missouri. In addition, we conducted car reconnaissance along 30 km of the river downstream from St. Charles. Exposure is very poor along this portion of the Missouri River due to erosion control measures including riprap and groins. The few exposures revealed laminated silt or interbedded silt and sand. We found no liquefaction features along the Missouri River.

Piasa Creek

We surveyed 8 km of Piasa Creek upstream from Lockhaven, Illinois. The upper portion of the creek had low, vegetated banks with poor exposure. The few small exposures we found revealed reddish silt overlying either layered silt or fine sand. Exposure improved along the lower portion of the creek. For a 1-km stretch, the creek flowed along the base of a very high cutbank in bedrock. Elsewhere, cutbanks ranged from 2 to 10 m in height and revealed primarily reddish silt overlying layered silt. At several locations, probing indicated that sand was interbedded with silt below water level. Despite poor exposure and less than ideal conditions for the formation of liquefaction features, we found one small sand dike (see Fig. 2 and Table 1). The sand dike was loose and fairly unweathered suggesting that it is probably Late Holocene in age.

Prairie du Pont Creek

Near Imbs and Tillman, Illinois, we surveyed 5 km of Prairie du Pont Creek, a tributary to the Mississippi River. The upper portion of the creek is incised in the uplands southeast of the Mississippi River floodplain. Many of the banks are low and vegetated and had been covered with recent flood deposits. The few exposures revealed weathered silt with only thin beds of sand. The lower 1 km of the creek flows across the margin of the Mississippi River floodplain and has been channelized. Exposure was poor except for the lower 1 m of the cutbank which

had been scoured. Along this reach, mottled silt is overlain by black clayey soils. Conditions did not appear suitable for the formation of liquefaction features.

Saline Creek

We surveyed 21 km of the lower Saline Creek, a tributary to the Mississippi River. All along the creek, bedrock outcrops intermittently. Along the upper 5 km, exposures reveal interbedded silt, gravel, and clay or silt and clay. Downstream, sand is occasionally interbedded with silt and clay. Along the lower 10 km, creek banks are slumped, vegetated, and poorly exposed. We found no liquefaction features along Saline Creek, but this is not surprising given the limited depth of unconsolidated sediments and the poor exposure along the lower reach of the stream.

Shoal Creek

We surveyed 20 km of the Shoal Creek between St. Rose and Breese, Illinois. Along the upper 12 km, bedrock outcrops intermittently. In a few places, interbedded clay, silt, and sand, overlie bedrock or diamicton. Elsewhere banks are vegetated, slumped, and generally poorly exposed. Exposure improves along the lower 8 km of the creek. Cutbanks are about 4 m high and expose mottled silt overlying interbedded silt and sand. We found three sand dikes at two sites along this stretch of the creek (see Fig. 2 and Table 1). All three sand dikes are small and occur in mottled silt that is probably Holocene in age. The dikes did not appear weathered but they occur low in the section. We found no material for dating at either site. Therefore, we have little control on the age estimate of the dikes.

Silver Creek

We surveyed 9 km of Silver Creek where it crosses the uplands adjacent to the Kaskaskia River floodplain. Along the upper 4 km of this portion of the creek, we encountered many exposures of bedrock and a few exposures of interbedded silt and sand. Downstream there were many good exposures of mottled silt overlying interbedded silt and sand and cross-bedded sand. Conditions are not suitable for the formation of liquefaction features along the upper portion of Silver Creek. Conditions are more suitable downstream, but we found no liquefaction features.

Richland Creek

We surveyed the lower 9 km of Richland Creek, a tributary to the Kaskaskia River. In general, exposure was poor, especially along the lower 6 km where banks have low slopes and are vegetated. A few small exposures and probing of cutbanks suggested that mottled silt is underlain by interbedded silt and sand. We found no liquefaction features but this is not surprising given the poor exposure.

Investigation of Meramec River Liquefaction Site MR25W

This liquefaction site (MR25W) previously found along the Meramec River was selected for further study because it is only 25 kilometers from downtown St. Louis, contains a 20-cm-wide sand dike, as well as several other smaller dikes, and possibly a sand blow (Fig. 2, see inset; and Fig. 4).

Careful examination revealed that the possible sand blow is actually a fluvial deposit (see Fig. 5; units 3a and 3b) that had been locally liquefied either by ground shaking or by water flow into

Figure 4. Photograph of 20 cm-wide pebbly, sand dike at MR25W about 25 km southwest of St. Louis along Meramec River. Weathering characteristics (fines accumulation and iron-staining) of sand dike suggest that it is prehistoric in age. Other sand dikes along Meramec River probably formed during 1811-1812 New Madrid earthquakes. Photo by M. Tuttle.

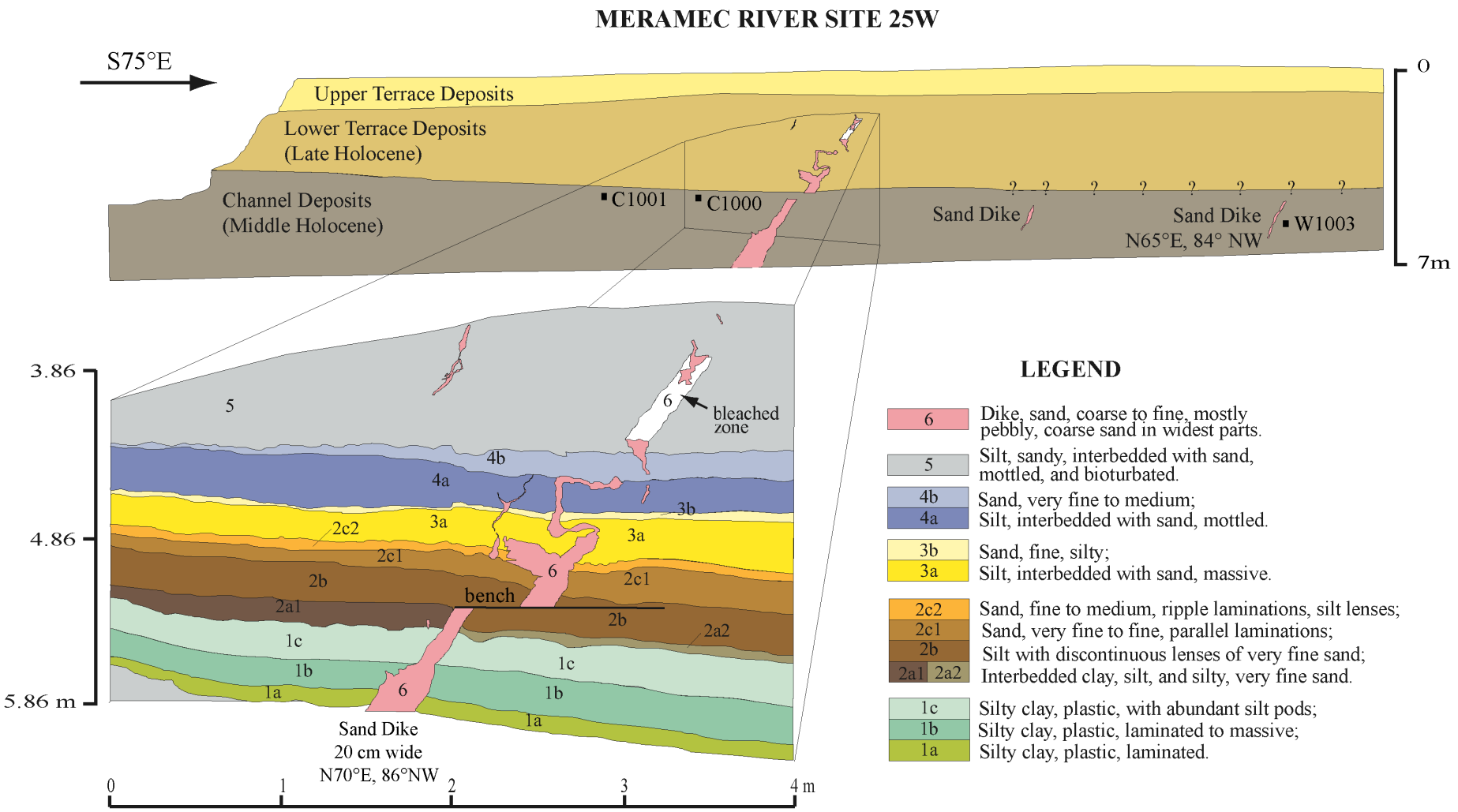

Figure 5. (Upper) Diagram of cutbank at MR25W showing major depositional units and location of sand dikes, charcoal (C#) and wood (W#) samples collected for radiocarbon dating, and logged area outlined by thin black lines. (Lower) Log of 20 cm-wide pebbly, sand dike and fluvial deposits that it intrudes. Sand dike is estimated to have formed during Late Holocene. Radiocarbon dating of channel deposits provides maximum age constraint indicating sand dike formed since 4340 B.C., and radiocarbon dating of lower terrace deposits at upstream site suggests that sand dike may have formed since 800 B.C. Log by M. Tuttle and J. Sims.

the layer via the sand dike. The 20-cm-wide sand dike crosscuts the sandy fluvial deposit and continues up-section for another meter where it terminates about 3.66 m below the top of the cutbank. Other smaller sand dikes terminate lower in the section and their relationship to the larger sand dike is unclear. The 20-cm-wide dike, in general, fines upward from pebbly, coarse sand in its lower section, to coarse-medium sand in its middle section, to fine sand towards its tip. Fines have accumulated in the upper 50 cm of the dike and the entire dike is either iron-stained or iron-cemented. Given its weathering characteristics, this feature probably is not historic in age. Unfortunately, samples for radiocarbon dating were found only in the channel deposits more than 1 meter below the dike tip. Therefore, the radiocarbon dates (see Fig. 5 and Table 2) provide only maximum age constraint for the 20-cm wide sand dike and indicate that it formed since 4340 B.C. At an archeological site upstream from MR25W, charcoal from a shell midden in the lower terrace deposits, like those at MR25W in which the sand dike terminates, yielded a calibrated date of 800-415 B.C. Therefore, it is possible, but be no means required, that the 20-cm wide sand dike formed during the Late Holocene.

This site illustrates the difficulty in estimating the ages of sand dikes. Rarely is it possible to determine close maximum or minimum age constraints for sand dikes. Until the age(s) of the liquefaction features at this site are better constrained, their correlations with other features across the region will have a high degree of uncertainty.

Analysis of Liquefaction Potential of MR25W

The Missouri Department of Transportation (MDOT) conducted *in situ* geotechnical testing, including two borings 4.57 m apart, at MR25W. According to the log of boring 1, which was closest to the sand dike, there are three sandy layers within 15 m (50 ft) of the ground surface (Table 3). These layers include fine sand from 3.7-5.4 m (12-17.6 ft) below the surface, gravelly sand from 9.5- 10.1 m (31-33 ft), and silty sand from 14.3-15.7 m (47-51.5 ft). The upper sandy layer was not observed in boring 2. The middle layer of sandy gravel at 9.5- 10.1 m below the surface seems the most likely source of the 20-cm wide sand dike for the following reasons. First, the sand dike originates below 7 m and crosscuts the deposit of interbedded sand and silty sand as observed in the cutbank exposure between 3.86-5.36 m below the ground surface (Figs. 4 and 5). Second, the pebbly, sand dike appears to more closely match the gravelly sand at 9.5-10.1 m than the silty sand at 14.3-15.7 m.

Using the standard penetration (SPT) data collected at the site, we evaluated scenario earthquakes (e.g., **M** 5.25, 6, 6.75, 7.5, 7.8, and 8 at distances of 10, 32, 40, 80, 100, 125, and 200 km) for possible source areas or known geologic structures, including the St. Louis fault, Centralia fault-Du Quoin monocline, and the New Madrid fault system (Fig. 1; Appendix II). In evaluating the scenario earthquakes, we employed the simplified procedure, also known as the cyclic stress method, of liquefaction potential analysis (e.g., Seed and Idriss, 1982; Youd et al., 2001). The procedure is relatively easy to apply and is suitable for many field and tectonic settings. Using appropriate ground motion relations (e.g., Atkinson and Boore, 1995), we estimated values of peak ground acceleration and calculated the cyclic stress ratio that would be generated by the various scenario earthquakes. Employing the empirical relation between cyclic stress ratio and corrected blow counts, we determined whether or not the three sandy layers at MR25W would be likely or not likely to liquefy during the earthquakes.

Table 3. Liquefiable Sediments at Meramec River Site 25W From MDOT Borings

Boring	Depth Suscep. Sediment (ft)	Blow Count (N)	Water Table (ft)	Description
B-1	16	2	15	Sand, fine with clay and trace silt, with thin layers of silty sand and clayey silt.
B-1	31	13	15	Gravelly sand, brown and gray, cherty gravel.
B-1	47	12	15	Silty sand, gray, some reddish-brown, with trace to some gravel and clay.
B-2	31	5	15	Sandy gravel with trace brown silt and silty sand.
B-2	37	10	15	Silty sand, gray, some reddish-brown, with trace to some gravel and clay.

According to our liquefaction potential analysis (see Appendix II), a local (within 10 km of MR25W) earthquake of **M** 5.25 would induce liquefaction in the upper layer (boring 1) and the middle layer (boring 2); whereas a local **M** 6.0 earthquake would induce liquefaction in all three layers. A **M** 6.75 earthquake centered in Germantown, Illinois (~80 km from the site), would not induce liquefaction in any of the sandy layers at the site; whereas a **M** 7.5 earthquake in Germantown would induce liquefaction in all but the lower layer in boring 2. Alternatively, a **M** 7.5 earthquake along the Centralia fault-Du Quoin monocline (~100 km from the site) would induce liquefaction in the uppermost layer (boring 1) and the middle layer (boring 2); whereas a **M** 7.8 earthquake along the same structure would induce liquefaction in all but the lower layer in boring 2. According to the analysis, a **M** 8 earthquake produced by the northern New Madrid fault system would not induce liquefaction at the site.

If only the middle layer is considered (since it appears to have been the source of the sand dike), the 20-cm wide sand dike could have formed as a result of (1) a local (within 10 km) earthquake of **M** 6.0, and possibly as small as 5.25, (2) a **M** 7.5 earthquake in Germantown, Illinois, or (3) an earthquake of **M** 7.8, and possibly as small as 7.5, along the Centralia fault-Du Quoin monocline (Appendix II). These results are similar to an earlier analysis using borehole data from a nearby bridge crossing of the Meramec River (Tuttle et al., 1999). This analysis does not take into account affects of site conditions on ground motions or changes in the liquefaction susceptibility of the sediments resulting from the event or since the event.

Uncertainties of Age Estimates of Liquefaction Features

We reviewed age estimates of previously and newly found liquefaction features and ranked the quality of the estimates (A-D) based on radiocarbon dating, maximum and minimum age

constraints of features, weathering characteristics of features, and dating at nearby sites (Appendix I). This evaluation makes explicit uncertainties in the age estimates and helps to identify areas where additional effort is needed to improve age estimates of liquefaction features. For example, age estimates for several Middle Holocene liquefaction features along Big Muddy and Kaskaskia Rivers and Shoal Creek are of high quality. However, age estimates of Middle Holocene features along the lower Cache River and Cahokia Creek are of poor quality. If Middle Holocene liquefaction features could be confidently correlated along all these rivers, the area of liquefaction associated with the 4520 B.C. ± 200 yr event would be greatly enlarged. Until the age estimates of the Middle Holocene liquefaction features along the lower Cache River are improved, they can be interpreted in several ways. They could have formed as a result of a very large earthquake originating from a distant source such as the NMSZ or a smaller magnitude earthquake from a closer source such as the Commerce Geophysical lineament.

Several liquefaction features along the Meramec River are estimated to have formed during the 1811-1812 earthquakes. These estimates are thought to be of high quality. Several other features along the Meramec are estimated to have formed during the Late Holocene and Holocene. These estimates are of moderate to poor quality, respectively. No liquefaction features along the Meramec has yet been attributed to the 4520 B.C. $\pm$ 200 yr earthquake. If this earthquake was centered near Germantown, Illinois, and did not induce liquefaction along the Meramec River, it is likely to have been of **M** < 7.5. Additional efforts to search for and improve age estimates of liquefaction features along the Cache, Meramec and other rivers in the region would help to test this and other hypotheses.

Conclusions

During this study, reconnaissance for liquefaction features was conducted along numerous rivers and creeks in the St. Louis region. Additional liquefaction features, interpreted as forming in 1811-1812 or during the Late Holocene, Middle Holocene, and Holocene, were found along the Kaskaskia and Meramec Rivers and Cahokia, Crooked, Piasa, and Shoal Creeks (Fig. 2). These findings indicate that the distribution of liquefaction features is greater than previously determined and that additional reconnaissance in the region is still warranted.

Detailed study of a liquefaction site on the Meramec River helped to ascertain that a discontinuous sandy layer crosscut by a 20-cm wide sand dike is not a sand blow. Unfortunately, only a maximum age estimate of 4340 B.C., and not even a close estimate, could be determined for the sand dike. Stratigraphic relations suggest that the sand dike might be as young as 800 B.C. Correlation of the 20-cm wide sand dike with other liquefaction features across the region is tenuous given the uncertainty in its age estimate. Liquefaction potential analysis suggests that the sand dikes at the Meramec River site could have formed as a result of a moderate to large earthquake centered in the St. Louis area or a very large earthquake centered 80 to 100 km east of St. Louis.

We reviewed age estimates of previously and newly found liquefaction features and ranked the quality of the estimates (A-D). The ranking illustrates the wide range of uncertainties in the age estimates of liquefaction features and points to particular events or geographical areas for which additional information is especially needed. Most of the paleoseismic data in the St. Louis

region are derived from reconnaissance-level studies. Estimates of timing of past earthquakes are based on well-constrained age estimates for only a few liquefaction features. Additional study and dating of liquefaction features is needed to further constrain the timing of paleoearthquakes and to make regional correlations of similar-age liquefaction features. A more complete picture of the size and spatial distributions of liquefaction features is needed to interpret the source areas and magnitudes of prehistoric earthquakes with greater confidence.

Acknowledgements

Research presented in this report was supported by grant 99HQGR0032 from the U.S. Geological Survey. The views and conclusions presented here are those of the author and should not be interpreted as necessarily representing official policies, either expressed or implied, by the U.S. Government. Kathleen Dyer-Williams performed the liquefaction potential analysis and John Sims, Dave Hoffman, and Ingrid Ekstrom participated in river reconnaissance. Dave Hoffman also provided geotechnical data from MDOT. Kathy Tucker compiled liquefaction data and produced the regional map of liquefaction sites. Permission to access and work at the Meramec River 25W and Cahokia Creek 2 liquefaction sites was kindly granted by Charles Forbis, Steve Creager, Thomas Allen, and George Willaredt.

References Cited

Ambraseys, N. N., 1988, Engineering Seismology: earthquake engineering and structural dynamics, Journal of the International Association of Earthquake Engineering, v. 17, p. 1-105.

Atkinson, G. M., and Boore, D. M., 1995, Ground-motions relations for eastern North America, Bulletin of the Seismological Society of America, v. 85, n. 1, p. 17-30.

Hajic, E. R., and Wiant, M. D., 1997, Dating of prehistoric of prehistoric earthquake liquefaction in southeastern and central Illinois, U.S. Geological Survey, Technical Report 57 p.

Harrison, R. W., 1997, Bedrock geologic map of the St. Louis 30 x 60 quadrangle, Missouri and Illinois, U.S. Geological Surv. Misc. Invest. Ser. Map I-2533, scale 1:100,000.

Johnston, A. C., and Schweig, E. S., 1996, The enigma of the New Madrid earthquakes of 1811-1812, Annual Review of Earth and Planetary Sciences, v. 24, p. 339-384.

McCracken, M. H., 1971, Structural features of Missouri: Mo. Geol. Surv. and Water Res., Rept. of Investigations v.49, 99 p., map.

McNulty, W. E., and Obermeier, S. F., 1999, Liquefaction evidence for at least two strong Holocene paleo-earthquakes in central and southwestern Illinois, USA, Environmental and Engineering Geoscience, v. 5, n. 2, p. 133-146.

Mitchell, B. J., Nuttli, O. W., Herrmann, R. B., Stauder, W., 1991, Seismotectonics of the central United States, *in* Slemmons, D.B., Engdahl, E.R., Zoback, M.D., and Blackwell, D.D., eds., Neotectonics of North America: Boulder, Colorado, Geol. Soc. Am. Decade Map Volumne 1, p. 245-260.

Munson, P. J., Obermeier, S. F., Munson, C. A., and Hajic, E. R., 1997, Liquefaction evidence for Holocene and Latest Pleistocene seismicity in the southern halves of Indiana and Illinois: A preliminary overview, Seism. Soc. of Am., v. 68, n. 4, p. 521-536.

Nuttli, O. and Brill, K., 1981, Earthquake source zones in the central United States determined from historical siesmicity, *in* Barstow, N.L., Brill, K.G., Nuttli, O.W., and Pomeroy, P.W., eds., Approach to seismic zonation for siting nuclear electric power generating facilities in the

eastern United States, US Nuclear Regulatory Commission Report NUREG/CR-1577, p. 98-143.
Obermeier, S. F., Martin, J. R., Frankel, A. D., Youd, T. L., Munson, P. J., Munson, C. A., and Pond, E. C., 1993, Liquefaction evidence for one or more strong Holocene earthquakes in the Wabash Valley of southern Indiana and Illinois, with a preliminary estimate of magnitude, U.S. Geological Survey, Professional Paper 1536, 27 p.
Olson, S. M., Green, R. A., Obermeier, S. F., 2004, Geotechnical analysis of paleoseismic shaking using liquefaction features: Part I. Major updating of techniques for analysis, U.S. Geological Survey Poen-File Report 03-307, 33 p.
Quinlan, G., 1987, Models of subsidence mechanisms in intracratonic basins, and their applicability to North American examples, *in* Beaumont, C., and Tankard, A. J., eds., Sedimentary Basins and Basin-Forming Mechanisms, Canad. Soc. of Petrol. Geol., Memr., 12, p. 463-481.
Saucier, R. T., 1991, Geoarchaeological evidence of strong prehistoric earthquakes in the New Madrid (Missouri) seismic zone, Geology, v. 19, p. 296-298.
Seed, H. B., and Idriss, I. M., 1982, Ground motions and soil liquefaction during earthquakes, Earthquake Engineering Research Institute, Berkley, 134 p.
Tuttle, M. P., Chester, J., Lafferty, R., Dyer-Williams, K., and Cande, R., 1999, Paleoseismology study northwest of the New Madrid seismic zone, NUREG/CR-5730, 96 p.
Tuttle, M. P., Schweig, E. S., Sims, J. D., Lafferty, R. H., Wolf, L. W., Haynes, M. L., 2002, The earthquake potential of the New Madrid seismic zone, Bulletin of the Seismological Society of America, v. 92, n. 6, p. 2080-2089.
Tuttle, M. P., Schweig, E., III, Campbell, J., Thomas, P. M., Sims, J. D., and Lafferty, R. H., III, 2005, Evidence for New Madrid earthquakes in A.D. 300 and 2350 B.C., Seismological Research Letters, v. 76, p. 489-501.
Youd, T. L., et al., 2001, Liquefaction resistence of soils: Summary report from the 1996 NCEER and 1998 NCEER/NSF workshops on evaluation of liquefaction resistence of soils, Journal of Geotechnical and Geoenvironmental Engineering, v. 127, n. 10, p. 817-833.

Appendix I. Liquefaction Features Found in St. Louis Region During This Study and Prior Study by Tuttle et al. (1999).

SITE NAME	NO. DIKE	DIKE WIDTH (CM)	DIKE STRIKE	DIKE DIP	SILL THICK-NESS (CM)	SILL LENGTH	OTHER DEFORMATION	C14 CONSTRAINT	C14 COMMENT	WC	AGE ESTIMATE	CERTAINTY
BC02							contorted bedding; folding; faulting				LW	D
BMR02					possible sill		faulting	28,330 BP	max	O	LWH	B
BMR02c	3	0.1- 1			12	300 cm	some	28,330 BP	max	O	LWH	B
BMR07							3 sand diapirs; 0.5 - 1cm	5590 BC	max (BMR09)		MH	C
BMR09	1	1	N34E	90			N	5590 BC	max	O	MH	B
BMR16							6 sand diapirs; 1 – 2 cm	8590 BC	max		MH	B
BMR17	several dikelets		N16E	87NW	24	not measured	N	9070 BC-4240 BC			MH	A
BR02							convoluted bedding; ball & pillow structures; sand diapirs	400-190 BC	max (BR01)		LH	C
BR07	1 possible dike	2					N	AD 1030-1260	host above		LH	B
BR105a							sand diapirs; slump	AD 1660-1950	1 m above	Y	LH	B
BR105b	possible dike				possible sill		sand diapirs; ball & pillow structures; minor load casts	AD 1660-1950	1 m above	Y	LH	B
BR107							load casts; sand diapirs; flow structure	AD 1500-1950	paleosol above	Y	LH	B
BR110							load casts; sand diapirs	AD 1310	max	Y	LH	B
BR21							sand diapirs; disturbed bedding			Y	LH	D
BR22							contorted bedding; load casts; small sand diapir			Y	LH	D
BR23							ball & pillow structures; deformed bedding			Y	LH	D
CahC02	1	35	N50°W	85°SW			N			O	LWH	D
CahC04a	3	1.25	N33°W	84°NE			N			O	MH	D
CahC04b		1	N38°W	87°NE			N			O	MH	D
CahC04c		0.5	N47°W	90°			N			O	MH	D
CahC05	1	1.5	N37°W	88°NE			N	160BC	max	Y	LH	B
CahC06a	2	1.5	N13°E	88°NW			N			O	MH	D
CahC06b		1	N28°E	88°SE			N			O	MH	D
CahC07a	2	6	N26°E	64°NW			N				H	D
CahC07b		4	N4°E	75°SE			N				H	D

Appendix I. Cont'd

SITE NAME	NO. DIKE	DIKE WIDTH (CM)	DIKE STRIKE	DIKE DIP	SILL THICK-NESS (CM)	SILL LENGTH	OTHER DEFORMATION	C14 CONSTRAINT	C14 COMMENT	WC	AGE ESTIMATE	CERTAINTY
CC04	1	14	N28E	subvertical			N			O	MH	D
CC05	1	4	N8W	89W	2	20 cm	N			O	MH	D
CC06a	2	6	N10E	86NW			N			O	MH	D
CC06b		0.2	N55E	85NW			N			O	MH	D
CC07a	2	1.5	N15E	87SE			N	4785BC	max	Y	LH	B
CC07b		1.5	N48W	sub-vertical			N	4785BC	max	Y	LH	B
CC08 (100)	1	5	N30E	80NW			N				H	D
CC09 (101)	1	3.5	N88E	80SE			N				H	D
CR100	1	7	N78E				N			O	MH	D
CR101	1	4	N65W				N			O	MH	D
CR102		0.01					small dikes and diapirs			O	MH	D
CR103a	3	3, 2, 9	N55E	85SE			N	AD1020	max	Y	LH	B
CR103b			N5E	80NW			N	AD1020	max	Y	LH	B
CR103c							N	AD1020	max	Y	LH	B
CR105							possible fault				CR-PCR	D
CR106							possible fault				Q	D
CR10a	2	1	N55W	85SW			N				H	D
CR10b		0.3	N68W	88NE			N				H	D
CR11	1 that feeds sill	5			8	100 cm	N				H	D
CSTD01	1 possible	1					N				H	D
KR04	1	5	N53W	85NE			N	4850BC	close max	O	MH	B
KR06a	5	8	N4W	80W			N			O	MH	D
KR06b					5	435 CM	N			Y	LH	D
KR06c		7	N30W	85NE			N			O	MH	D
KR06d		5	N10E	90			N			O	MH	D
KR06e		2.5	N40E	82NW			N			O	MH	D
KR06f		1	N17E	90			N			O	MH	D
KR07a	2	11	N53W	8NE	9	not measured	flow structure in source sand	6720BC	max	O	MH	B
KR07b		9	N25W	90			flow structure in source sand	6720BC	max	O	MH	B
KR08	1	1	N80W	76N			N			Y	LH	D
KR10							sand diapirs; load casts; disturbed bedding; faulting				H	D

Appendix I. Cont'd

SITE NAME	NO. DIKE	DIKE WIDTH (CM)	DIKE STRIKE	DIKE DIP	SILL THICK-NESS (CM)	SILL LENGTH	OTHER DEFORMATION	C14 CONSTRAINT	C14 COMMENT	WC	AGE ESTIMATE	CERTAINTY
KR11a	2	20	N15W	86SW			N			O	MH	D
KR11b		2.5	N25E	90			N			O	MH	D
KR12a	2	3	N50E	76NW			N			O	MH	D
KR12b		2	N72E	88NW			N			O	MH	D
KR13a	2	1	N35W	90			N			O	MH	D
KR13b		1	N53W	90			N			O	H	D
KR15a	4	10	N83W	90			N			O	MH	D
KR15b		2.5	N50E	90			N			O	MH	D
KR17a	4	2	N46E	82SE			N	4800BC	max	Y	LH	B
KR17b		2	N45E	85SE			N	4800BC	max	Y	LH	B
KR17c		1	N32E	89SE			N	4800BC	max	Y	LH	B
KR17d		1	N46E	84SE			N	4800BC	max	Y	LH	B
KR18a	2	10	N15W	88SW			N	13700BP	max	O	LWH	B
KR18b		4	N9W	90			N	13700BP	max	O	LWH	B
KR19	2	6, 3	N60W	76SW	3 cm thick dike becomes sill		flow structure	1990BC	max	Y	LH	B
KR20	1	26+	N70W (N58 - 82W)	85NE			N	1990BC	max (KR19)	Y	LH	C
KR21a	2	4	N80W	83N			N			Y	LH	D
KR21b		3	N73W	83SW			N			Y	LH	D
KR22a(200)	8	7	N10E	85SE	possible sills		N	7495BC	max	O	MH	B
KR22b(200)		3	N40E	72NW			N	7495BC	max	O	MH	B
KR23a(201)	5	6	N15W	78SW			N			O	MH	D
KR23b(201)		4	N9E	84NW			N			O	MH	D
KR23c(201)		3	N3E	85SE						Y	LH	D
MAR01	1	0.5	N10W	85SW			N	3360BC	max	Y	LH	B
MAR03	3	5, 2, 0.5	N10W	90			N			Y	LH	D
MAR04	2 possible	1	N80W	90			N			Y	LH	D
MC07	1	7	N55W	81NE	6	not measured	N	5980BC	max	O	MH	B
MER22	1 dikelet	0.3					contorted & disturbed bedding; load casts	AD 1830	max	Y	1811-1812	B
MER22E	1	0.5	N42E	90			N	AD 1830	max (MER22)	Y	1811-1812	C

Appendix I. Cont'd

SITE NAME	NO. DIKE	DIKE WIDTH (CM)	DIKE STRIKE	DIKE DIP	SILL THICK-NESS (CM)	SILL LENGTH	OTHER DEFORMATION	C14 CONSTRAINT	C14 COMMENT	WC	AGE ESTIMATE	CERTAINTY
MER25	1	8	N53E	88NW			N	4340BC	(MER25W)		LH	C
MER25Wa	4	20	N70E	86NW	possible sill		N	4340BC	800BC possible max from MER202	O	LH	B
MER25Wb		1	N75EN	N52E			N	4340BC	800BC possible max from MER203		LH	B
MER25Wc	1	1	N45E	87SE			N	4340BC	800BC possible max from MER204	O	LH	B
MER26	1	3	S54W	60NW			N	4340BC	(MER25W)		LH	C
MER27	1	0.4					N				H	D
MER3a (203)	2	8	N81E	65SE			flow structure in dike	AD1670	max	Y	1811-1812	A
MER3b (203)		6	N32E	82NW				AD1670	max	Y	1811-1812	A
PC01	1	5	N80W	59N			N	2890BC	max		LH	B
PC02a	5	3	N45W	86SW			N	3340BC	max		LH	B
PC02b		1.5	N72E	78SE			N	3340BC	max		LH	B
PC06					sills		contorted bedding				H	D
PC08	5 dikelets	5, 2			8	100+ cm	distrubed bedding			Y	LH	D
PC09							possible faulting				Plio-Pleistocenc	D
PIcS02	1	1.5	N58W	85SW			N			Y	LH	D
SAC04							sand diapirs; load casts; disturbed bedding				H	D
SAC10							ball & pillow structures				H	D
SHC01	1	4	N2W	78NE			N	3630-3340BC	above dike	O	MH	B
SHC02	1	45	N67E	77SW			N	4940BC	max	O	MH	B
SHC04	1	18	N83W	88SW			N			O	MH	C
SHC05	1	3	N23W	90			N			O	MH	C
SHC06	1	155	N43W	90			N	4370BC	min	O	MH	B
SHC07a	6	4	N12E	84NW			N			O	MH	D
SHC07b		2	N23W	86SW			N			O	MH	D
SHC07c		1	N28W	90			N			O	MH	D
SHC09	3	5, 1, 1	N63W	87SW			N	5310BC	max	O	MH	B

Appendix I. Cont'd

SITE NAME	NO. DIKE	DIKE WIDTH (CM)	DIKE STRIKE	DIKE DIP	SILL THICK-NESS (CM)	SILL LENGTH	OTHER DEFORMATION	C14 CONSTRAINT	C14 COMMENT	WC	AGE ESTIMATE	CERTAINTY
SHC09	3	5, 1, 1	N63W	87SW			N	5310BC	max	O	MH	B
SHC100	2	1					N				H	D
SHC101	1	3	N80E	80SE			N				H	D
SHC10a	3	6	N36E	85NW			flow structure in dike	4680BC	max	O	MH	B
SHC10b		3	N75E	85NW			flow structure in dike	4680BC	max	O	MH	B
SHC10c		1	N38E	90			flow structure in dike	4680BC	max	O	MH	B
SHC11	1	0.5	N6E	89E			disturbed bedding in source sand			Y	LH	D
SIC101	1	1	N82W	90			N			Y	LH	D
SIC30							sand diapirs; load casts; slump				H	D

Explanation:

1. (WC) weathering characteristics: O -relatively old feature with fines accumulation and mottling; Y - relatively young feature, fairly clean and loose.
2. A - certain based on both minimum and maximum age constraints of feature or maximum constraint on historic feature;
   B - fairly certain based on dating at site and weathering characteristics of feature;
   C - somewhat certain based on dating at nearby site and weathering characteristics of feature;
   D - uncertain based on general understanding of age of host deposit and weathering characteristics of feature.

Key to Site Names:

BC- Beaucoup Creek; BMR- Big Muddy River; BR- Big River; CahC- Cahokia Creek; CC- Crooked Creek; CR- Cache River; CSTD- Castor River Diversion Channel; KR- Kaskaskia River; MAR- Marys River; MC- Mud Creek; MER- Meramec River; PC- Post Creek; PIcS- Piasa Creek; SAC- Saline Creek; SHC- Shoal Creek; SiC- Silver Creek.

Appendix II. Liquefaction Potential Analysis for Sediments at Meramec River Site 25W.

Boring	Depth (ft)	M[1]	Distance	a_{max}[2]	$N_{1(60)}$[3]	Cyclic Stress Ratio[4]	Results[5]
B-1	16	5.25	10	0.27	2	0.159	L
B-1	31	5.25	10	0.27	9	0.180	N
B-2	31	5.25	10	0.27	3	0.180	L
B-2	37	5.25	10	0.27	11	0.179	N
B-1	47	5.25	10	0.27	7	0.170	N
B-1	16	5.25	32	0.09	2	0.053	N
B-1	31	5.25	32	0.09	9	0.060	N
B-2	31	5.25	32	0.09	3	0.060	N
B-2	37	5.25	32	0.09	11	0.060	N
B-1	47	5.25	32	0.09	7	0.057	N
B-1	16	6	10	0.51	2	0.300	L
B-1	31	6	10	0.51	9	0.341	L
B-2	31	6	10	0.51	3	0.341	L
B-2	37	6	10	0.51	11	0.338	L
B-1	47	6	10	0.51	7	0.322	L
B-1	16	6	32	0.16	2	0.035	N
B-1	31	6	32	0.16	9	0.107	N
B-2	31	6	32	0.16	3	0.107	L
B-2	37	6	32	0.16	11	0.106	N
B-1	47	6	32	0.16	7	0.101	N
B-1	16	6	40	0.12	2	0.007	N
B-1	31	6	40	0.12	9	0.080	N
B-2	31	6	40	0.12	3	0.080	N
B-2	37	6	40	0.12	11	0.080	N
B-1	47	6	40	0.12	7	0.076	N
B-1	16	6.75	40	0.22	2	0.130	L
B-1	31	6.75	40	0.22	9	0.147	N
B-2	31	6.75	40	0.22	3	0.147	L
B-2	37	6.75	40	0.22	11	0.146	N
B-1	47	6.75	40	0.22	7	0.139	L

Appendix II. Cont'd

Boring	Depth (ft)	M[1]	Distance	a_{max}[2]	$N_{1(60)}$[3]	Cyclic Stress Ratio[4]	Results[5]
B-1	16	6.75	80	0.08	2	0.047	N
B-1	31	6.75	80	0.08	9	0.053	N
B-2	31	6.75	80	0.08	3	0.053	N
B-2	37	6.75	80	0.08	11	0.053	N
B-1	47	6.75	80	0.08	7	0.050	N
B-1	16	7	40	0.27	2	0.157	L
B-1	31	7	40	0.27	9	0.178	L
B-1	47	7	40	0.27	7	0.168	L
B-1	16	7	80	0.10	2	0.059	M/L
B-1	31	7	80	0.10	9	0.067	N
B-1	47	7	80	0.10	7	0.063	N
B-1	16	7	100	0.08	2	0.044	N
B-1	31	7	100	0.08	9	0.050	N
B-1	47	7	100	0.08	7	0.048	N
B-1	16	7.5	40	0.40	2	0.236	L
B-1	31	7.5	40	0.40	9	0.267	L
B-2	31	7.5	40	0.40	3	0.267	L
B-2	37	7.5	40	0.40	11	0.265	L
B-1	47	7.5	40	0.40	7	0.252	L
B-1	16	7.5	80	0.17	2	0.094	L
B-1	31	7.5	80	0.17	9	0.107	L
B-2	31	7.5	80	0.17	3	0.107	L
B-2	37	7.5	80	0.17	11	0.106	N
B-1	47	7.5	80	0.17	7	0.101	L
B-1	16	7.5	100	0.12	2	0.065	L
B-1	31	7.5	100	0.12	9	0.074	N
B-2	31	7.5	100	0.12	3	0.074	L
B-2	37	7.5	100	0.12	11	0.073	N
B-1	47	7.5	100	0.12	7	0.069	N
B-1	16	7.5	125	0.08	2	0.047	N
B-1	31	7.5	125	0.08	9	0.053	N
B-2	31	7.5	125	0.08	3	0.053	N

Appendix II. Cont'd

Boring	Depth (ft)	M[1]	Distance	a_{max}[2]	$N_{1(60)}$[3]	Cyclic Stress Ratio[4]	Results[5]
B-2	37	7.5	125	0.08	11	0.053	N
B-1	47	7.5	125	0.08	7	0.050	N
B-1	16	7.8	80	0.20	2	0.117	L
B-1	31	7.8	80	0.20	9	0.133	L
B-2	31	7.8	80	0.20	3	0.133	L
B-2	37	7.8	80	0.20	11	0.132	L
B-1	47	7.8	80	0.20	7	0.126	L
B-1	16	7.8	100	0.14	2	0.085	L
B-1	31	7.8	100	0.14	9	0.096	L
B-2	31	7.8	100	0.14	3	0.096	L
B-2	37	7.8	100	0.14	11	0.096	N
B-1	47	7.8	100	0.14	7	0.091	L
B-1	16	7.8	125	0.10	2	0.061	L
B-1	31	7.8	125	0.10	9	0.069	N
B-2	31	7.8	125	0.10	3	0.069	L
B-2	37	7.8	125	0.10	11	0.068	N
B-1	47	7.8	125	0.10	7	0.065	N
B-1	16	7.8	200	0.05	2	0.029	N
B-1	31	7.8	200	0.05	9	0.033	N
B-2	31	7.8	200	0.05	3	0.033	N
B-2	37	7.8	200	0.05	11	0.033	N
B-1	47	7.8	200	0.05	7	0.031	N
B-1	16	8	80	0.23	2	0.138	L
B-1	31	8	80	0.23	9	0.156	L
B-2	31	8	80	0.23	3	0.156	L
B-2	37	8	80	0.23	11	0.155	L
B-1	47	8	80	0.23	7	0.148	L

Appendix II. Cont'd

Boring	Depth (ft)	M[1]	Distance	a_{max}[2]	$N_{1(60)}$[3]	Cyclic Stress Ratio[4]	Results[5]
B-1	16	8	100	0.17	2	0.100	L
B-1	31	8	100	0.17	9	0.113	L
B-2	31	8	100	0.17	3	0.113	L
B-2	37	8	100	0.17	11	0.112	L
B-1	47	8	100	0.17	7	0.107	L
B-1	16	8	125	0.12	2	0.071	L
B-1	31	8	125	0.12	9	0.081	L
B-2	31	8	125	0.12	3	0.081	L
B-2	37	8	125	0.12	11	0.081	N
B-1	47	8	125	0.12	7	0.077	L
B-1	16	8	200	0.06	2	0.034	N
B-1	31	8	200	0.06	9	0.039	N
B-2	31	8	200	0.06	3	0.039	N
B-2	37	8	200	0.06	11	0.039	N
B-1	47	8	200	0.06	7	0.037	N

Key
[1]M – moment magnitude of the earthquake
[2]amax – maximum acceleration at ground surface
[3]N_1 – corrected blow count (N) from the standard penetration test (SPT)
[4]Cyclic Stress Ratio – stress causing liquefaction